Journal of Solid Mechanics Vol. 6, No. 2 (2014) pp. 173-193

Nonlinear Nonlocal Vibration of an Embedded Viscoelastic Y-SWCNT Conveying Viscous Fluid Under Magnetic Field Using Homotopy Analysis Method

A. Ghorbanpour Arani[1,2 *], M.SH. Zarei[1]

[1]*Faculty of Mechanical Engineering, University of Kashan, Kashan, Islamic Republic of Iran*
[2]*Institute of Nanoscience & Nanotechnology, University of Kashan, Kashan, Islamic Republic of Iran*

Received 3 March 2014; accepted 30 April 2014

ABSTRACT

In the present work, effect of von Karman geometric nonlinearity on the vibration characteristics of a Y-shaped single walled carbon nanotube (Y-SWCNT) conveying viscose fluid is investigated based on Euler Bernoulli beam (EBB) model. The Y-SWCNT is also subjected to a longitudinal magnetic field which produces Lorentz force in transverse direction. In order to consider the small scale effects, nonlocal elasticity theory is applied due to its simplicity and accuracy. The small-size effects and slip boundary conditions of nano-flow are taken into account through Knudsen number (Kn). The Y-SWCNT is surrounded by elastic medium which is simulated as nonlinear Visco-Pasternak foundation. Using energy method and Hamilton's principle, the nonlinear governing motion equation is obtained. The governing motion equation is solved using both Galerkin procedure and Homotopy analysis method (HAM). Numerical results indicate the significant effects of the mass and velocity of the fluid flow, strength of longitudinally magnetic field, (Kn), angle between the centerline of carbon nanotube and the downstream elbows, nonlocal parameter and nonlinear Visco-Pasternak elastic medium. The results of this work is hoped to be of use in design and manufacturing of nano-devices in which Y-shaped nanotubes act as basic elements.

Keywords: Homotopy analysis method; Nonlinear visco-pasternak foundation; Viscose fluid flow; Y-SWCNT; Knudsen number (Kn)

1 INTRODUCTION

CARBON nanotubes (CNTs) which were discovered by Iijima [1] have widespread applications in different fields such as chemistry, physics, engineering, material science and reinforced composite structures. This is largely due to the combination of desirable characteristics, such as structural perfection, small size, low density, high stiffness, high strength and excellent electronic properties. CNTs possess extraordinary physical properties, such as high stiffness-to-weight and strength-to-weight ratios, and high electrical and thermal conductivities compared to any other known material. It is commonly believed in the scientific community that nanotechnology will spark a series of industrial revolutions in the following decades. The discovery of CNTs has been a very significant breakthrough that has accelerated further developments in the field of nanotechnology. CNTs are among the most promising new materials and are expected to play a pivotal role in the future of nanotechnology.

* Corresponding author. Tel.: +98 361 5912450; Fax: +98 361 5912424.
E-mail address: aghorban@kashanu.ac.ir (A. Ghorbanpour Arani).

In order to investigate the mechanical behaviors of nano-structures, the higher order continuum theories which are scale dependent theories such as nonlocal elasticity [2-5], nonlocal piezoelasticity [6-9], modified couple stress theory [10-13] and strain gradient theory [14,15] have been recently employed. It is because the classical theory is a scale independent theory and cannot handle the small scale effects. Among these, nonlocal elasticity theory which was first introduced by Eringen [16] has been widely utilized to study the mechanical manner in the micron and nano scale structures. There are many works in the literature that have used this theory. Based on nonlocal elasticity theory Wang and Wang [2] investigated the vibration of nanotubes embedded in an elastic matrix using Timoshenko beam (TB) model. They showed that the obtained frequencies have a significant dependence on the nonlocal parameter. Fang et al. [3] studied the nonlinear free vibration of double-walled carbon nanotubes (DWCNTs) based on the nonlocal elasticity theory. Their results showed the importance of nonlocal parameter on the vibration characteristics of DWCNTs. Analytical solutions for bending and buckling of functionally graded nanobeams based on the nonlocal TB theory was presented by Simsek and Yurtcu [4].

In recent years, a large amount research works have been carried out on the buckling and vibration of the nanotubes/microtubes conveying fluid [17-20]. Also, the dynamic response of viscous fluid conveying nanotubes has been reported by several investigators [21-24]. Their results show the effect of fluid viscosity on dynamical behavior of nanotubes. For instance, Abdollahian et al. [22] investigated the nonlocal wave propagation in embedded armchair three-walled boron nitride nanotubes conveying viscous fluid. In another attempt, vibration analysis of a viscous-fluid-conveying single-walled carbon nanotube (SWCNT) embedded in an elastic medium was studied by Lee and Chang [23]. On the other hand, Rashidi et al. [25] demonstrated that the small-size effects on the flow cannot be ignored and should be considered in nano-scale fluid structure interaction problems. For this purpose they used (Kn) as a discriminant parameter to consider both small-size effects on bulk viscosity and slip boundary conditions of nanoflow. Also, Mirramezani and Mirdamadi [26] investigated the effect of nano-size of both fluid flow and elastic structure simultaneously on the vibrational behavior of a pinned-pinned and a clamped-clamped nanotube conveying fluid, using both (Kn) and nonlocal continuum theory.

In nanoscale problems, surface-to-bulk energy ratio increases; therefore surface effects must be taken into account while they can be disregarded in macroscopic structural problems. Based on TB theory and surface elasticity model, Lei et al. [27] analyzed the vibrational behavior of (DWCNTs). Asgharifard Sharabiani and Haeri Yazdi [28] studied the nonlinear vibration of functionally graded nanobeams with surface effects within the framework of EBB theory including the von Karman geometric nonlinearity. An analytical model for predicting surface effects on the free vibration of fluid-conveying nanotubes was developed by Wang [29] based on nonlocal elasticity theory. He demonstrated that surface effect is significant especially for smaller tube thicknesses or larger aspect ratios.

Multi-terminal nanotube junctions, namely junctions of L, X, Y, and T-types, have recently attracted much attention in nanotransistors and nanoamplifiers. Among different types of nanotube junction T- and Y-junctions have received increasingly attention. A (Y-SWCNT) is a novel structure consisting of three terminals with different chirality [30]. Y-shaped nanotubes exhibit electronic properties that are improved conventional transistors used in computers. Indeed, the discovery of Y-shaped carbon nanotubes represents a new way of thinking about nano-electronic devices.

The foundation of CNTs can be assumed as Winkler, Pasternak and Visco-Pasternak medium. Since Winkler model considers only the parameter representing the normal pressure, it cannot be considered as a precise approximation. On the other hand, Pasternak foundation considers both shear and normal loads. In this paper, in order to come closer to the physical reality, the nonlinear Visco-Pasternak elastic medium is assumed. Lin [31] studied nanoscale vibration characterization of multi-layered graphene sheets embedded in an elastic medium. He modeled the elastic foundation as Pasternak foundation and concluded that increasing the shear modulus factor of elastic medium increases the classical natural frequency of the system. Small scale effect on vibration of multilayered graphene sheets embedded on Pasternak foundation was investigated by Pradhan and Phadikar [32]. Ghorbanpour Arani et al. [33] presented the nonlinear vibration of (DWCNTs) embedded on Pasternak elastic medium and subjected to an axial fluid flow. In another attempt, Ghorbanpour Arani et al. [34] carried out the electro-thermal vibration of double boron nitride nanotubes which are coupled by Visco-Pasternak elastic foundation. Also, the surrounding elastic medium can be assumed as linear or nonlinear foundations. In another study, Eichler et al. [35] investigated the nonlinear damping in mechanical resonators made from carbon nanotubes.

The governing differential equations can be solved using different analytical and numerical solution methods. The (HAM) is a numerical method that is employed to solve the governing nonlinear differential equations. This method is used in many works to solve the nonlinear differential equations. Pirbodaghi et al. [36] used HAM to investigate nonlinear vibration behavior of EBB subjected to axial loads. They compared results obtained by HAM with those available in literature and demonstrated the accuracy of HAM. Moghimi Zand and Ahmadian [37] also

used HAM in studying dynamic pull-in instability of microsystems. They considered different sources of nonlinearity such as electrostatic force and mid-plane stretching.

Therefore, according to the best of author's knowledge and the above discussion, it is so clear that no work has been reported concerning the vibration of Y-SWCNTs. On the other hand, Y-SWCNTs can be used in many nanoelectromechanical systems (NEMS) and the problem of vibration analysis of Y-SWCNTs conveying viscose fluid becomes more useful in medical fields and nanodevices. Motivated by these considerations we aim to study nonlinear nonlocal vibration of a viscoelastic single-walled carbon nanotube conveying viscous fluid with the Y-shaped junction piece at the downstream end under magnetic field. The Y-SWCNT embedded on a nonlinear Visco-Pasternak elastic medium. The governing nonlinear differential equations obtained by energy method and Hamilton's principle, are then solved using Galerkin method and HAM as well. The effects of the longitudinally magnetic field, Y-junction piece at the downstream end, slip boundary condition, small scale parameter, fluid flow and elastic foundation are presented graphically.

2 FORMULATION

2.1 Preliminaries

Consider a Y-SWCNT covered by a thin outer surface layer conveying viscose fluid as shown in Fig. 1. The Y-SWCNT is modeled as EBB with a tubular cross section of inner radius R_i , outer radius R_0 , thickness h_t , length L and the angle between the centerline of the CNT and the downstream elbows ϕ indicated in Fig. 1. The Y-SWCNT is rested on an elastic medium which is simulated by a nonlinear visco-pasternak foundation and also is subjected to a longitudinally magnetic field. It should be noted that the length of Y-junction fitted at downstream is assumed to be small and may be ignored. For EBB model, the nonlinear strain-displacement relationships of von Karman type along the x and z axes for an arbitrary point are defined by $\tilde{U}(x,z,t)$ and $\tilde{W}(x,z,t)$ respectively as follows:

$$\tilde{U}(x,z,t) = u(x,t) - z\frac{\partial w(x,t)}{\partial x}, \tag{1a}$$

$$\tilde{W}(x,z,t) = w(x,t), \tag{1b}$$

$$\varepsilon_{xx} = \frac{\partial u}{\partial x} + \frac{1}{2}\left(\frac{\partial w}{\partial x}\right)^2 - z\frac{\partial^2 w}{\partial x^2}, \tag{2}$$

where x is the longitudinal coordinate, z is the coordinate measured from the mid-plane of the beam. The terms $u(x,t)$ and $w(x,t)$ are the longitudinal and transverse components of the displacement in the mid-plane of the beam, respectively.

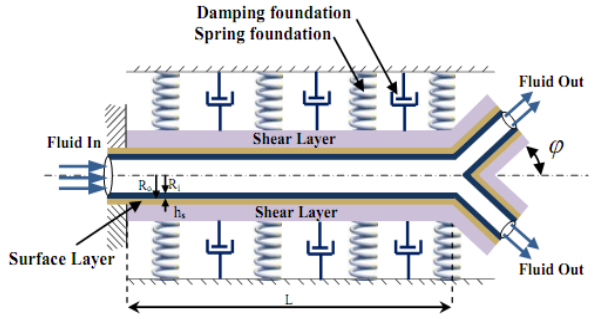

Fig. 1
Configuration of embedded Y-SWCNT conveying fluid.

2.2 Strain energy

The strain energy of the Y-SWCNT U , can be expressed as:

$$U = \frac{1}{2}\int_0^L \int_{A_t} \sigma_{xx}\varepsilon_{xx} dx dA_t , \tag{3}$$

In which σ_{xx} is the axial classical stress and A_t is the cross sectional area of the SWCNT. Substituting Eq. (2) into Eq. (3) yields:

$$U = \frac{1}{2}\int_0^L \left[N_x \left(\frac{\partial u}{\partial x} + \frac{1}{2}\left(\frac{\partial w}{\partial x} \right)^2 \right) - M_x \frac{\partial^2 w}{\partial x^2} \right] dx , \tag{4}$$

where N_x , M_x are the resultant force and moment resultant, respectively and are defined as:

$$N_x = \int_{A_t} \sigma_{xx} dA_t , M_x = \int_{A_t} \sigma_{xx} z dA_t . \tag{5}$$

2.3 Kinetic energies
2.3.1 Kinetic energy of Y-SWCNT

The kinetic energy of Y-SWCNT K_t , can be written as follows:

$$K_t = \frac{1}{2}\int_0^L \int_{A_t} \left(\rho_t + \rho_e \delta(x - L) \right) \left(\left(\frac{\partial \tilde{U}}{\partial x} \right)^2 + \left(\frac{\partial \tilde{W}}{\partial x} \right)^2 \right) dx dA_t , \tag{6}$$

where ρ_t , ρ_e and δ are the mass density of Y-SWCNT, mass density of the downstream Y-junction and Dirac delta function, respectively.

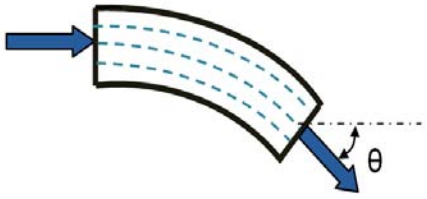

Fig. 2
An element of nanotube conveying fluid.

2.3.2 Kinetic energy of fluid flow

The kinetic energy associated with the fluid flow K_f , can be expressed as:

$$K_f = \frac{1}{2}\int_0^L \int_{A_f} \rho_f \left(\vec{v}^2 + z^2 \left(\frac{\partial w}{\partial x} \right)^2 \right) dx dA_f , \tag{7}$$

In which ρ_f and A_f are the mass density and cross sectional area of fluid flow, respectively. According to Fig. 2 and considering small-size effects on slip boundary conditions of nano-flow, the velocity vector of fluid flow $\vec{v}$ can be written as [38]:

$$\vec{v} = \left(U^* \cos\theta + \frac{\partial u\left(x,t\right)}{\partial t} \right)\vec{i} + \left(-U^* \sin\theta + \frac{\partial w\left(x,t\right)}{\partial t} \right)\vec{j}, \quad \theta = -\frac{\partial w}{\partial x}, \tag{8}$$

where U^* is average flow velocity with slip boundary condition and can be defined as:

$$U^* = \gamma U, \tag{9}$$

where U denotes the average flow velocity through Y-SWCNT without slip boundary conditions and the average velocity correction factor γ can be defined as follows [25]:

$$\gamma = \left(1 + aKn\right)\left(4\left(\frac{2-\sigma_v}{\sigma_v} \right)\left(\frac{Kn}{Kn+1} \right) + 1 \right), \tag{10}$$

In which the tangential moment accommodation coefficient σ_v is equal to 1 , a is a coefficient which is defined as:

$$a = a_0 \frac{2}{\pi} \tan^{-1}(a_1 Kn^B), \tag{11}$$

where $a_1 = 4$ and $B = 0.4$ are some empirical parameters and a_0 can be obtained from free molecular regime as:

$$\lim a_{Kn\to\infty} \equiv a_0 = \frac{64}{3\pi(1-\frac{4}{b})}, \tag{12}$$

where for the second-order slip boundary conditions *b* is equal to -1.

2.3.3 Kinetic energy of the fluid flow at the downstream Y-junction

Also the kinetic energy of the fluid flow at downstream Y-junction K_{fe} is defined as:

$$K_{fe} = \frac{1}{2}\int_0^L \int_{A_{fe}} \rho_{fe} \vec{v}^2 \delta\left(x - L\right) dA_{fe} dx, \tag{13}$$

In which A_{fe} and ρ_{fe} are the cross sectional area and the mass density of the Y-junction.

2.4 External forces

The Y-SWCNT conveying viscous fluid is subjected to a longitudinally magnetic field and embedded on nonlinear Visco-Pasternak elastic medium. Also an additional bonded thin surface layer (outer layer) is encompassed the Y-SWCNT. Therefore, the following five external effects should be considered to obtain the energy of virtual works:

- Viscous fluid flow
- Fluid flow at downstream Y-junction
- Magnetic field
- Nonlinear Visco-Pasternak foundation
- Surface effects

2.4.1 Viscous fluid flow

To investigate the effect of fluid viscosity on the vibration behaviors of Y-SWCNT, the well-known Navier-Stockes equation is used as [21]:

$$\rho_f \frac{d\vec{v}}{dt} = -\nabla p + \mu_e \nabla^2 \vec{v}, \tag{14}$$

In which p is pressure, ∇^2 is defined as $\partial^2/\partial x^2$ and μ_e is the effective viscosity of the nano-fluid which is defined as follows:

$$\mu_e = \mu_0 \left(\frac{1}{1+aKn} \right), \tag{15}$$

where μ_0 is the bulk viscosity.

Substituting Eq. (8) into Eq. (14) and using Eq. (9) yields:

$$\rho_f \left[\frac{\partial}{\partial t} + \gamma U \frac{\partial}{\partial x} \right] \left[\frac{\partial u}{\partial t} + \gamma U \cos\theta \right] = -\frac{\partial p}{\partial x} + \mu_e \frac{\partial^2}{\partial x^2} \left[\frac{\partial u}{\partial t} + \gamma U \cos\theta \right], \tag{16a}$$

$$\rho_f \left[\frac{\partial}{\partial t} + \gamma U \frac{\partial}{\partial x} \right] \left[\frac{\partial w}{\partial t} - \gamma U \sin\theta \right] = -\frac{\partial p}{\partial z} + \mu_e \frac{\partial^2}{\partial x^2} \left[\frac{\partial w}{\partial t} - \gamma U \sin\theta \right]. \tag{16b}$$

Applying surface integrals ($m_f = \int_{A_f} \rho_f dA_f$) to Eqs. (16), the viscosity terms were derived and added to the equation of motion.

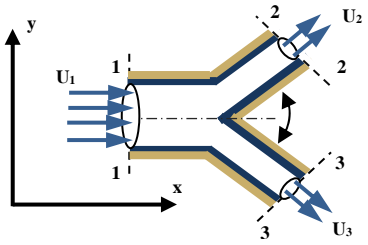

Fig. 3
The control volume of fluid flow at downstream Y-junction.

2.4.2 Fluid flow at downstream Y-junction

On the other hand, tensile forces along the axial and transverse directions $\left(F_x \text{ and } F_y\right)$ exert to the Y-SWCNT due to the fluid flow at the Y-junction. In order to obtain work done by these forces, the famous momentum equation for the incoming fluid flow at section 1-1 and out coming fluid flow at sections 2-2 and 3-3 is used according to Fig. 3:

$$\begin{aligned} F_x &= \rho_f Q_3 (U^{*3})_x + \rho_f Q_2 \left(U^{*2}\right)_x - \rho_f Q_1 \left(U^{*1}\right)_x = 2\rho_f Q_2 \left(U^{*2}\right)_x - \rho_f Q_1 \left(U^{*1}\right)_x = \\ &\rho_f Q_1 \left(U^{*2}\right)_x - \rho_f Q_1 \left(U^{*1}\right)_x = \rho_f Q_1 \left(\left(U^{*2}\right)_x - \left(U^{*1}\right)_x \right) = \rho_f Q_1 \gamma \left(\left(U^{2}\right)_x - \left(U^{1}\right)_x \right), \end{aligned} \tag{17a}$$

$$F_y = \rho_f Q_3 \left(U^{*3}\right)_y + \rho_f Q_2 \left(U^{*3}\right)_y - \rho_f Q_1 \left(U^{*1}\right)_y = \rho_f Q_3 \left(-U^{*1} \sin\phi\right)_x + \rho_f Q_2 \left(U^{*1} \sin\phi\right)_x = 0, \tag{17b}$$

where $Q_i \ (i=1,2,3)$ is the volume flow rates. Also $U^{*i} \ (i=1,2,3)$ and $U^{i} \ (i=1,2,3)$ are the mean flow velocities at the relevant section with and without slip boundary conditions, respectively. Using Eqs. (17), the work done by the fluid flow at the downstream Y-junction can be written as:

$$V_{fe} = \frac{1}{2}\int_0^L m_f \ (\gamma U)^2 (1-\cos\phi)\frac{\partial^2 w}{\partial x^2} w dx . \tag{18}$$

2.4.3 Magnetic field

The governing electrodynamics Maxwell equations for a perfectly conducting, elastic body are given by Ghorbanpour Arani and Amir [39]. Imposing a magnetic field vector in longitudinal direction $\vec{H} = (H_x, 0, 0)$, assuming , therefore the Lorentz body force can be obtained as [39]:

$$F_m = \eta\left(\vec{J}\times\vec{H}\right) \Rightarrow F_m = \eta H_x^2 \left(\frac{\partial^2 w}{\partial x^2}\right). \tag{19}$$

Finally, the works done by the longitudinally magnetic field is written as follows:

$$V_m = \frac{1}{2}\int_0^L \left(-\eta A_t H_x^2 \left(\frac{\partial^2 w}{\partial x^2}\right)\right) w dx . \tag{20}$$

2.4.4 Nonlinear Visco-Pasternak foundation

Based on nonlinear Visco-Pasternak foundation, the effects of the surrounding elastic medium on the Y-SWCNT are considered as follows [34,35]:

$$V_e = \frac{1}{2}\int_0^L \left(-k_w w + G\nabla^2 w - c\frac{\partial w\ (x,t)}{\partial t}\right) w dx , \tag{21}$$

where k_w is the spring constant of the Winkler type, G is the shear constant of the Pasternak type and c is the nonlinear damper modulus which is defined in Eq. (46).

2.4.5 Surface effects

Since at nanoscale problems the ratio of surface-to-volume becomes significant, the effects of surface layer cannot be ignored. On the other hand, in this study an additional bonded thin surface layer (outer layer) is encompassed the Y-SWCNT for modeling the Y-SWCNT properly. For the surface of elastic material, the following basic relation can be written as[40]:

$$\tau_{\alpha\beta} = \gamma\delta_{\alpha\beta} + \frac{\partial \Gamma}{\partial \varepsilon_{\alpha\beta}}, \quad (\alpha,\beta = 1,2), \tag{22}$$

where $\tau_{\alpha\beta}$ is the surface stress tensor, γ is surface residual energy in the absence of external loading and surface deformation and Γ denotes the induced surface energy. Applying the Hook's law in the Eq. (22) yields the following stress-displacement relation as [40]:

$$\tau_{\alpha\beta} = \tau\delta_{ij} + \lambda^s \varepsilon_{\eta\eta}\delta_{\alpha\beta} + 2\mu^s \varepsilon_{\alpha\beta}, \quad (i,j = 1,2,3), \tag{23}$$

In which λ^s and μ^s are the Lame constants of surface material, and τ denotes the surface residual stress. The generalized Young-Laplace equation can be written in the cases with zero thickness as follows:

$$\Delta\sigma_{ij} n_i n_j = \tau_{\alpha\beta}\kappa_{\alpha\beta}, \tag{24}$$

where $\Delta\sigma_{ij}$ is the stress jump across each external interface surface, n_i is the unit normal vector and $\kappa_{\alpha\beta}$ is the curvature tensor.

It is assumed that the thickness of the surface layer h^s is much smaller than the thickness h_t and inner radius R_i of Y-SWCNT. It is assumed that the thickness of the thin surface layer approaches zero; hence, the Laplace-Young equations [29] can be used to express the surface residual stress as:

$$\tau_{xz} = 4\tau_0 R_o \frac{\partial^2 w}{\partial x^2}, \tag{25}$$

In which τ_0 is the residual surface tension. Also, the work done by the resulting distributed transverse loading induced by surface effects can be written as follow:

$$V_s = \frac{1}{2}\int_0^L 4\tau_0 R_0 \frac{\partial^2 w}{\partial x^2} w dx. \tag{26}$$

Considering the additional axial flexural rigidities due to outer surface layer and using the composite beam theory [41] yields the effective flexural rigidity as:

$$(EA)^* = EA + 2E^s \pi t^s R_o, \tag{27a}$$

$$(EI_t)^* = EI_t + E^s \pi h^s R_o^3, \tag{27b}$$

where E^s and E is the Young's modulus of surface layer and Y-SWCNT, respectively.

2.5 Hamilton's principle

The motion equations of embedded Viscoelastic Y-SWCNT conveying viscous fluid can be derived using Hamilton's principle as follows:

$$\int_0^t \delta\left(U - K_t - K_f - K_{fe} - V_{fe} - V_m - V_e - V_s\right)dt = 0. \tag{28}$$

Therefore, the motion equation for transverse vibration of an embedded Y-SWCNT conveying viscous fluid flow is derived as:

$$\begin{aligned}
&-\frac{\partial^2 M_x}{\partial x^2} + \left(m_t + m_f + m_{fe}\delta(x-L) + m_e\delta(x-L)\right)\frac{\partial^2 w}{\partial t^2} + 2U\left(m_f + m_{fe}\delta(x-L)\right)\frac{\partial^2 w}{\partial t\,\partial x}\cos\theta - \mu A_f \frac{\partial^3 w}{\partial x^2 \partial t} \\
&-\mu A U \frac{\partial^3 w}{\partial x^3}\cos\theta + U\left(m_f + m_{fe}\delta(x-L)\right)\frac{\partial^2 w}{\partial x^2}\frac{\partial w}{\partial t}\sin\theta - U\left(m_f + m_{fe}\delta(x-L)\right)\frac{\partial^2 w}{\partial x^2}\frac{\partial u}{\partial t}\cos\theta \\
&+U\left(m_f + m_{fe}\delta(x-L)\right)\frac{\partial^2 u}{\partial x\,\partial t}\sin\theta - \left(\rho_t I_t + \rho_f I_f\right)\frac{\partial^4 w}{\partial t^2 \partial x^2} - \mu A_f U\left(\frac{\partial^2 w}{\partial x^2}\right)^2 \sin\theta - \frac{EA}{2L}\frac{\partial^2 w}{\partial x^2}\int_0^L \left(\frac{\partial w}{\partial x}\right)^2 dx \\
&+(k_w w - G\nabla^2 w + c\frac{\partial w}{\partial t} + m_f U^2\cos\theta - m_f U^2(1-\cos\phi) - \eta H_x^2 A - 4\tau R_0)\frac{\partial^2 w}{\partial x^2} = 0.
\end{aligned} \tag{29}$$

3 NONLOCAL ELASTICITY THEORY BASED ON KELVIN'S MODEL

Based on nonlocal elasticity theory, the stress tensor at a reference point depends not only on the strain components at the same point but also on all other points of the body. Therefore, The constitutive equation of the nonlocal elasticity can be written as [3]:

$$\left(1-(e_0 a)^2\nabla^2\right)\sigma^{nl}=\sigma^{l}, \tag{30}$$

where ∇^2 is the Laplacian operator in the above. Based on Kelvin's model on elastic materials and EBB assumption, Eq. (30) can be rewritten as follows:

$$\sigma_{xx}-e_0^2 a^2\frac{\partial^2\sigma_{xx}}{\partial x^2}=E\left(1+g\frac{\partial}{\partial t}\right)\left(\frac{\partial u}{\partial x}-z\frac{\partial^2 w}{\partial x^2}+\frac{1}{2}\left(\frac{\partial w}{\partial x}\right)^2\right), \tag{31}$$

where E and g are the Young's modulus and damping coefficient of Y-SWCNT, respectively. Also σ_{xx} and ε_{xx} are the longitudinal stress and strain components, respectively. Using Eqs. (5) and (31) yields the force and moment resultants as follows:

$$N_x-e_0^2 a^2\frac{\partial^2 N_x}{\partial x^2}=EA^*\frac{\partial u}{\partial x}+EA^* g\frac{\partial^2 u}{\partial x\,\partial t}, \tag{32a}$$

$$M_x-e_0^2 a^2\frac{\partial^2 M_x}{\partial x^2}=-EI^*\frac{\partial^2 w}{\partial x^2}-EI^* g\frac{\partial^3 w}{\partial x^2\partial t}, \tag{32b}$$

where the additional axial $(EA)^*$ and flexural $(EI_t)^*$ rigidities can be obtained from Eqs. (27).

4 MOTION EQUATIONS

The following non-dimensional parameters can be defined for generality of the solution as:

$$\begin{aligned}
&\bar{x}=\frac{x}{L},\bar{w}=\frac{w}{L},\bar{h}=\frac{E^s\pi t^s R_o^3}{EI_t},\bar{\tau}=\frac{4\tau R_o}{A_t E},\bar{\varepsilon}=\frac{2E^s t^s R_0}{E(R_o{}^2-R_i{}^2)},\bar{G}=\frac{G}{A_t E},\ \bar{K}_w=\frac{K_w L^4}{EI_t},\bar{\xi}=\frac{A_t L^2}{I_t},\\
&\bar{U}=\sqrt{\frac{m_f}{EI_t}}U^*L,\bar{g}=g\sqrt{\frac{EI_t}{m_f+m_t}}\frac{1}{L^2},\beta=\frac{\mathrm{m}_f}{m_f+m_t},\bar{\beta}_f=\frac{m_{fe}}{L\sqrt{m_f^2+m_f m_t}},\bar{\beta}_{fe}=\frac{m_{fe}+m_e}{L\sqrt{m_f+m_t}},\\
&\bar{\mu}_e=\frac{\mu_e A_f}{\sqrt{EI_t\ \mathrm{m}_f}},\bar{e}_n=\frac{e_0 a}{L},\bar{c}=\frac{cL^2}{\sqrt{(m_f+m_t)EI_t}},\bar{t}=\sqrt{\frac{EI_t}{m_f+m_t}}\frac{t}{L^2},\bar{\sigma}=\frac{\rho_t I_t+\rho_f I_f}{L^2(m_f+m_t)},\bar{H}_x=\frac{1}{E}\eta H_x^2.
\end{aligned} \tag{33}$$

Substituting Eqs. (32) into Eq. (29) and using Eq. (33), the following dimensionless motion equation for transverse vibration of Y-SWCNT can be written as:

$$\bar{\sigma}\bar{e}_n^2\frac{\partial^6\bar{w}}{\partial\bar{t}^2\partial\bar{x}^4}+\left[\bar{g}\left(1+\bar{h}\right)-\bar{e}_n^2\bar{\mu}_e\left(1+\bar{\varepsilon}\right)\sqrt{\bar{\beta}}\right]\frac{\partial^5\bar{w}}{\partial\bar{x}^4\partial\bar{t}}-\bar{e}_n^2\bar{\mu}_e\left(1+\bar{\varepsilon}\right)\bar{U}\frac{\partial^5\bar{w}}{\partial\bar{x}^5}-$$
$$2\bar{e}_n^2\bar{U}\left[\sqrt{\bar{\beta}}+\bar{\beta}_f\,\delta\left(\bar{x}-1\right)\right]\frac{\partial^4\bar{w}}{\partial\bar{t}\,\partial\bar{x}^3}-\left[\bar{\sigma}+\bar{e}_n^2\left(1+\bar{\beta}_{fe}\delta\left(\bar{x}-1\right)\right)\right]\frac{\partial^4\bar{w}}{\partial\bar{x}^2\partial\bar{t}^2}+$$
$$\left[1+\bar{h}-\bar{e}_n^2\left[\bar{U}^2\cos\phi-\bar{\xi}\left(\bar{H}_x\left(1+\bar{\varepsilon}\right)+\bar{\tau}+\bar{G}+\frac{1}{2}\left(1+\bar{\varepsilon}\right)\int_0^1\left(\frac{\partial\bar{w}}{\partial\bar{x}}\right)^2d\bar{x}\right)\right]\right]\frac{\partial^4\bar{w}}{\partial\bar{x}^4}-$$
$$\left[\bar{\mu}_e\left(1+\bar{\varepsilon}\right)\sqrt{\bar{\beta}}+\bar{e}_n^2\bar{c}+4\bar{e}_n^2\bar{\beta}_f\bar{U}\frac{\partial\delta\left(\bar{x}-1\right)}{\partial\bar{x}}\right]\frac{\partial^3\bar{w}}{\partial\bar{x}^2\partial\bar{t}}-\left(1+\bar{\varepsilon}\right)\bar{\mu}_e\bar{U}\frac{\partial^3\bar{w}}{\partial\bar{x}^3}+\left[1+\bar{\beta}_{fe}\delta\left(\bar{x}-1\right)\right]\frac{\partial^2\bar{w}}{\partial\bar{t}^2}+$$
$$\left[\bar{U}^2\cos\phi-\bar{\xi}\left(\bar{H}_x\left(1+\bar{\varepsilon}\right)+\bar{\tau}+\bar{G}+\frac{1}{2}\left(1+\bar{\varepsilon}\right)\int_0^1\left(\frac{\partial\bar{w}}{\partial\bar{x}}\right)^2d\bar{x}\right)-\bar{e}_n^2\bar{K}_w\right]\frac{\partial^2\bar{w}}{\partial\bar{x}^2}+\bar{c}\frac{\partial\bar{w}}{\partial\bar{t}}+\bar{K}_w\bar{w}+$$
$$2\bar{U}\left[\sqrt{\bar{\beta}}+\bar{\beta}_f\,\delta\left(\bar{x}-1\right)-\bar{e}_n^2\bar{\beta}_f\frac{\partial^2\delta\left(\bar{x}-1\right)}{\partial\bar{x}^2}\right]\frac{\partial^2\bar{w}}{\partial\bar{t}\,\partial\bar{x}}=0. \tag{34}$$

5 SOLUTION METHOD

5.1 Galerkin method

In this article, the Galerkin method is used to convert the Eq. (34) into an ordinary differential equation form. The dimensionless transverse displacement can be assumed as:

$$\bar{w}\left(\bar{x},\bar{t}\right)=\sum_{i=1}^{N}\varphi_i T_i\left(\bar{t}\right), \tag{35}$$

In which $T_i\left(\bar{t}\right)$ is the dynamic response of the Y-SWCNT and $\varphi_i\left(\bar{x}\right)$ is the orthogonal function which should satisfy the boundary conditions. For the mechanical clamped-free boundary conditions assumed in this paper, one can consider the following equation as:

$$\varphi_i\left(\bar{x}\right)=\sin\left(\lambda_i\bar{x}\right)-\sinh\left(\lambda_i\bar{x}\right)+\frac{\sinh\lambda_i-\sin\lambda_i}{\cosh\lambda_i+\cos\lambda_i}\left[\cosh\left(\lambda_i\bar{x}\right)-\cos\left(\lambda_i\bar{x}\right)\right], \tag{36}$$

In which λ_i is the dimensionless fundamental frequency.

Also for different boundary conditions, the following equation may be used:

$$\frac{\partial^4\varphi_i}{\partial\bar{x}_i^{\,4}}=\lambda_i^4\varphi_i\,. \tag{37}$$

The C-F boundary conditions at both ends of Y-SWCNT are written in dimensionless form as [42]:

$$\varphi_i\left(0\right)=\frac{\partial\varphi_i\left(0\right)}{\partial\bar{x}}=0,\frac{\partial^2\varphi_i\left(1\right)}{\partial\bar{x}^2}=\frac{\partial^3\varphi_i\left(1\right)}{\partial\bar{x}^3}=0. \tag{38}$$

Furthermore, the *n*th derivative of Dirac-delta function $\delta^{(n)}\left(.\right)$ in Eq. (34), can be eliminated by applying the following property as:

$$\int_{x_1}^{x_2} g(x)\delta^{(n)}(x-x_0)dx = \begin{cases} (-1)^n g^{(n)}(x_0) & if\ x_1 < x_0 < x_2 \\ 0 & Otherwise \end{cases}. \tag{39}$$

Substituting Eq. (35) into Eq. (34), applying Eqs. (36) to (39), multiplying the obtained relation by φ_j and integrating over the length of the nanotube yields:

$$[M]\frac{\partial^2 T_i}{\partial \bar{t}^2} + [C]\frac{\partial T_i}{\partial \bar{t}} + [K]T_i + [N]T_i^3 = 0, \tag{40}$$

where $[K]$, $[C]$, $[M]$ and $[N]$ are the linear stiffness matrix, damping matrix, mass matrix and nonlinear stiffness matrix, respectively.

5.2 Homotopy analysis method

In this section, an introduction about a general analytic method which is called (HAM) is presented. HAM basically aims to solve nonlinear ordinary differential equations by transforming a nonlinear problem into an infinite number of linear problems.

Consider the following relation which is was constructed by Liao [43] as:

$$\bar{H}\left(\Phi,q,h,H(\tau)\right) = (1-q)L\left[\Phi(\tau,q) - u_0(\tau)\right] - qhH(\tau)N\left[\Phi(\tau,q)\right], \tag{41}$$

In which Φ is a function of t and q, h is a non-zero auxiliary parameter, $H(\tau)$ is a non-zero auxiliary function and L is an auxiliary linear operator. Also q is an auxiliary parameter increases from zero to one. It is worth mentioning that the solution varies from initial approximation to the exact solution as q increases from zero to one. Setting $\bar{H}\left(\Phi,q,h,H(\tau)\right) = 0$, the following equation can be concluded as:

$$(1-q)L\left[\Phi(\tau,q) - u_0(\tau)\right] = qhH(\tau)N\left[\Phi(\tau,q)\right]. \tag{42}$$

The initial conditions of Eq. (42) can be assumed as:

$$\Phi(0,q) = a, \frac{d\Phi(0,q)}{dt} = 0. \tag{43}$$

On the other hand, applying Taylor's theorem yields the following expansions as:

$$\Phi(\tau,q) = \Phi(\tau,0) + \sum_{m=1}^{\infty} \frac{1}{m!}\frac{\partial^m \Phi(\tau,q)}{\partial q^m}\bigg|_{q=0} q^m = u_0(\tau) + \sum_{m=1}^{\infty} u_m(\tau)q^m, \tag{44a}$$

$$\omega(q) = \omega_0 + \sum_{m=1}^{\infty} \frac{1}{m!}\frac{\partial^m \omega(q)}{\partial q^m}\bigg|_{q=0} q^m = \omega_0 + \sum_{m=1}^{\infty} \omega_m q^m. \tag{44b}$$

According to this method, Eq. (40) can be rewritten for the first mode ($N = 1$) as follows:

$$\mathbf{M}\ddot{T} + \mathbf{C}\dot{T} + \mathbf{K}T + \mathbf{N}\mathbf{L}T^3 = 0. \tag{45}$$

In this study, the surrounded elastic medium is assumed to be nonlinear; therefore, the nonlinear damper modulus of elastic medium (c) mentioned in Eq. (21), is considered as the following form:

$$c = c_1 + c_2 T^2. \tag{46}$$

Therefore, one can rewrite matrix $\left[C_{ij}\right]$ in Eq. (40) as follows:

$$\mathbf{C} = \left[C_{ij}\right] = C_{11} = C_1 + C_2 T^2, \tag{47}$$

In which:

$$\begin{aligned} C_1 = &\left[\bar{g}(1+\bar{h}) - \bar{e}_n^2 \bar{\mu}_e \left(1+\bar{\varepsilon}\right)\sqrt{\bar{\beta}}\right]\lambda_1^4 - 2\bar{e}_n^2 \bar{U}\sqrt{\bar{\beta}}\int_0^1 \frac{\partial^3 \varphi_1}{\partial \bar{x}^3}\varphi_1 d\bar{x} - \bar{\mu}_e\left(1+\bar{\varepsilon}\right)\sqrt{\bar{\beta}}c_{11} \\ &- \bar{\mu}_e\left(1+\bar{\varepsilon}\right)\bar{U}\int_0^1 \frac{\partial^3 \varphi_1}{\partial \bar{x}^3}\varphi_1 d\bar{x} + 2\bar{U}\sqrt{\bar{\beta}}b_{11} + 2\bar{U}\bar{\beta}_f \frac{\partial \varphi_1(1)}{\partial \bar{x}}\varphi_1(1) - (\bar{e}_n^2 c_{11} - 1)\bar{c}_1, \end{aligned} \tag{48a}$$

$$C_2 = (\bar{e}_n^2 c_{11} - 1)\bar{c}_2 T^2. \tag{48b}$$

Therefore, one can rewrite Eq. (45) as:

$$\ddot{T} + \left(\mathbf{C}_1 + \mathbf{C}_2 T^2\right)\dot{T} + \Omega_L^2 T + \Omega_{NL}^2 T^3 = 0, \tag{49}$$

where $\Omega_L = \mathbf{K}/\mathbf{M}, \Omega_{NL} = \mathbf{NL}/\mathbf{M}, \mathbf{C}_1 = C_1/\mathbf{M}$ and $\mathbf{C}_2 = C_2/\mathbf{M}$. Introducing $\tau = \omega t$ and $T\left(t\right) = u\left(\tau\right)$, Eq. (50) can be concluded from Eq. (49) as:

$$\omega^2 u''(\tau) = f\left[u(\tau), \omega u'(\tau), \omega^2 u''(\tau)\right]. \tag{50}$$

with the following initial conditions:

$$u(0) = a, u'(0) = 0, \tag{51}$$

where a and ω are the amplitude and frequency of motion.

Since free vibration of a system is a periodic motion, the following base functions can be assumed as [44]:

$$\left\{\sin(m\tau), \cos(m\tau) \qquad m = 1,2,3,\ldots\right\} \Rightarrow u(\tau) = \sum_{k=0}^{\infty}\left(c_k \sin m\tau + d_k \cos m\tau\right), \tag{52}$$

In which c_k and d_k are unknown coefficients. Choosing the following initial guess of $u\left(\tau\right)$ for zero-order deformation equation , the initial conditions are satisfied, therefore:

$$u_0(\tau) = a\cos\tau. \tag{53}$$

Based on the relation presented in Eq. (52), the auxiliary linear operator L can be chosen as:

$$L\left[\phi(\tau,q)\right]=\omega_0^2\left[\frac{\partial^2\Phi(\tau,q)}{\partial\tau^2}+\Phi(\tau,q)\right]. \tag{54}$$

Also the nonlinear operator can be defined from Eq. (50) as follows:

$$N\left[\Phi(\tau,q),\omega(q)\right]=\omega^2(q)\frac{\partial^2\Phi(\tau,q)}{\partial^2\tau}-f\left[\Phi(\tau,q),\omega(q)\frac{\partial\Phi(\tau,q)}{\partial\tau},\omega^2(q)\frac{\partial^2\Phi(\tau,q)}{\partial^2\tau}\right]. \tag{55}$$

$$\Phi(\tau,0)=u_0(\tau),\omega(0)=\omega_0. \tag{56}$$

It is while when q increasing from zero to one, $\Phi(\tau,q)$ varies from initial approximation $u_0(\tau)=a\cos\tau$ to the exact solution $u(\tau)$ and also $\Phi(\tau,q)$ changes from initial approximation ω_0 to the exact value of frequency.

Using Eqs. (44) and (56) yields the following relations as:

$$\Phi(\tau,q)=u_0(\tau)+\sum_{m=1}^{\infty}u_m(\tau)q^m,\omega(q)=\omega_0+\sum_{m=1}^{\infty}\omega_m q^m, \tag{57}$$

In which:

$$u_m(\tau)=\frac{1}{m!}\frac{\partial^m\Phi(\tau,q)}{\partial q^m}\bigg|_{q=0},\omega_m=\frac{1}{m!}\frac{\partial^m\omega(q)}{\partial q^m}\bigg|_{q=0}. \tag{58}$$

Differentiating Eqs. (42) and (43) m times with respect to the q and setting $q=0$, yields the m-order deformation equation as:

$$L\left[u_m(\tau)-x_m u_{m-1}(\tau)\right]=hH(\tau)R_m(\vec{u}_{m-1},\vec{\omega}_{m-1}). \tag{59}$$

with the following boundary conditions:

$$u_m(0)=a_m,u_m'(0)=0,x_m=\begin{cases}0 & m\le 1\\ 1 & otherwise\end{cases}. \tag{60}$$

also,

$$R_m(\vec{u}_{m-1},\vec{\omega}_{m-1})=\frac{1}{(m-1)!}\frac{d^{m-1}N\left[\Phi(\tau,q),\omega(q)\right]}{dq^{m-1}}\bigg|_{q=0},\vec{u}_{m-1}=\{u_0,u_1,u_2,\ldots,u_{m-1}\}, \tag{61}$$

$\vec{\omega}_{m-1}=\{\omega_0,\omega_1,\omega_2,\ldots,\omega_{m-1}\}$.

Considering Eq. (52) , the following relation may be obtained as:

$$R_m(\vec{u}_{m-1},\vec{\omega}_{m-1})=\sum_{n=0}^{m}b_{m,n}(\vec{\omega}_{m-1},\vec{u}_{m-1})\cos(2n+1)\tau+c_{m,n}(\vec{\omega}_{m-1},\vec{u}_{m-1})\sin(2n+1)\tau. \tag{62}$$

Using nonlinear operator from Eq. (55) , the following relation may be written as:

$$N\left[u\left(\tau,q\right),\omega\right]=\omega^2\left(q\right)\frac{\partial^2 u\left(\tau,q\right)}{\partial\tau^2}+C_1\omega\left(q\right)\frac{\partial u\left(\tau,q\right)}{\partial\tau}+C_2\omega\left(q\right)u^2\left(\tau,q\right)\frac{\partial^2 u\left(\tau,q\right)}{\partial\tau^2}+\Omega^2 u\left(\tau,q\right)+Nu\left(\tau,q\right). \tag{63}$$

Using Eqs. (61) and (63) ,the following equation can be expressed as:

$$\begin{aligned}R_m(u_{m-1},a_{m-1},\omega_{m-1})&=\frac{1}{(m-1)!}\times\frac{\partial^{m-1}N\left[u(\tau,q),\omega(q)\right]}{\partial q^{m-1}}\Big|_{q=0}=\sum_{m=0}^{m-1}(\sum_{j=0}^{n}\omega_j\times\omega_{n-j})u''_{m-1-n}+C_1\times\sum_{i=0}^{m-1}(\omega_i\times u''_{m-1-i})\\&+C_2\times\sum_{n=0}^{m-1}(\sum_{i=0}^{n}\omega_{n-i}\times\sum_{r=0}^{i}u_{i-r})\times\sum_{j=0}^{m-n-1}u_j\times u_{m-1-n-j}+\Omega^2\times u_{m-1}+N\times\sum_{n=0}^{m-1}(\sum_{j=0}^{n}u_j\times u_{n-j})\times u_{m-1-n}.\end{aligned} \tag{64}$$

It should be noted that the secular terms will appear in the final solution if the coefficient of $\sin\tau$ and $\cos\tau$ set to zero. Assuming $u_0\left(\tau\right)=a\cos\tau$ in Eq. (64) the following equation can be obtained for R_1 as:

$$R_1=(-\omega^2{}_0a_0+\Omega^2a_0+\frac{3}{4}N^3a_0)\cos(\tau)+(-C_1\omega_0a_0-\frac{1}{4}C_2\omega_0a^3{}_0)\sin(\tau)+\frac{1}{4}Na^3{}_0\cos(3\tau)-\frac{1}{4}C_2\omega_0a^3{}_0\sin(3\tau). \tag{65}$$

Setting the coefficient of $\sin\tau$ and $\cos\tau$ to zero , yields the following relations:

$$-C_1\omega_0a_0-\frac{1}{4}C_2\omega_0a^3{}_0=0,-\omega^2{}_0a_0+\Omega^2a_0+\frac{3}{4}N^3a_0=0. \tag{66}$$

Solving Eqs. (66) results:

$$a_0=\pm2\sqrt{-\frac{C_1}{C_2}},\qquad\omega_0=\frac{1}{2}\sqrt{4\Omega^2+3Na^2{}_0}\rightarrow\omega_0=\sqrt{\Omega^2-3N\frac{C_1}{C_2}}, \tag{67}$$

In which $C_1C_2<0$. Using Eqs. (59) and (60), one can obtain the following differential equation as:

$$u_1''(\tau)+u_1(\tau)=\frac{h}{\omega^2{}_0}R_1,\qquad u_1(0)=a_1,u_1''(0)=0. \tag{68}$$

Form Eq. (68), $u_1\left(\tau\right)$ can be derived as:

$$u_1(\tau)=-\frac{3}{32}\frac{ha^3{}_0C_2}{\omega_0}\sin(\tau)+\frac{1}{32}\frac{32a_1\omega^2{}_1+ha^3{}_0N}{\omega^2{}_0}\cos(\tau)+\frac{1}{32}\frac{ha^3{}_0C_2}{\omega_0}\sin(3\tau)+\frac{1}{32}\frac{ha^3{}_0N}{\omega^2{}_0}\cos(3\tau). \tag{69}$$

In order to obtain the coefficient a_1, R_2 may be written as follows:

$$R_2=\omega^2{}_0u_1''+2\omega_0u''_0\omega_1+C_1\omega_0u'_1+C_1\omega_1u'_0+2C_2\omega_0u_1u_0u'_0+C_2u^2{}_0\omega_1u'_0+C_2u^2{}_0\omega_0u'_1+\Omega^2u_1+3Nu^2{}_0u_1. \tag{70}$$

Therefore:

$$a_1=-\frac{1}{4}h\frac{\sqrt{-\frac{C_1}{C_2}}C_1N}{3C_1N-\Omega^2C_2},\qquad\omega_1=-\frac{1}{16}h\frac{C_1{}^2(C_2{}^2\Omega^2-3C_1C_2N+9N^2)}{(\Omega^2C_2+3C_1N)/C_2\times\sqrt{-\frac{-\Omega^2C_2+3C_1N}{C_2}}}. \tag{71}$$

Substituting Eqs. (63) and (71) into Eq. (69) yields $u_1(\tau)$. Also, the higher order approximations can be obtained similarly. For the second approximation, first $u_2(\tau)$ should be derived from Eqs. (59) and (60) as:

$$u_2'' + u_2 = \frac{h}{\omega_0^2}(R_1 + R_2), \qquad u_2(0) = a_2, u_2'(0) = 0. \tag{72}$$

Using Eq. (64), one can obtain the following relation for R_3 as:

$$\begin{aligned} R_3 &= 2\omega_2\omega_0 u_0'' + \omega_1^2 u_0'' + 2\omega_1\omega_0 u_1'' + \omega_0^2 u_2'' + C_1\omega_2 u_0' + C_1\omega_1 u_1' + C_1\omega_0 u_2' + C_2\omega_2 u_0' u_0^2 + C_2\omega_1 u_1' u_0^2 \\ &+ 2C_2\omega_1 u_0' u_0 u_1 + C_2\omega_0 u_2' u_0^2 + 2C_2\omega_0 u_1' u_0 u_1 + C_2\omega_0 u_0' u_1^2 + 2_1 C_2\omega_0 u_0' u_0 u_2 + \Omega^2 u_2 + 3N u_1^2 u_0 + 3N u_0^2 u_2. \end{aligned} \tag{73}$$

Setting the coefficients of $\sin\tau$ and $\cos\tau$ to zero, the following equation may be obtained as:

$$\begin{aligned} a_2 = -\frac{1}{64}\Bigg[& C_1 h\sqrt{-\frac{C_1}{C_2}}(216N^3C_1^2 + 171C_1^2 hN^3 - 129N^2 C_1\Omega^2 C_2 h \\ & -144N^2 C_1\Omega^2 C_2 + 10N^2 C_1 hk + 24N^2 C_1 k + 12NhC_2 C_1^2 k - 8NhC_2\Omega^2 k - 8NC_2\Omega^2 k \\ & +24NC_2^2\Omega^2 + 24NC_2^2\Omega^4 h - 4hC_2^2 C_1\Omega^2 k\Big)\Bigg] / \Big[k\left(C_2^2\Omega^4 - 6C_2\Omega^2 C_1 N + 9N^2 C_2^2\right)\Big], \end{aligned} \tag{74a}$$

$$\begin{aligned} \omega_2 = -\frac{C_1^2 h}{512}\Bigg[& 324N^3 C_1^3 C_2 hk - 9N^2 C_1^4 hC_2^2 k - C_1^2 hC_2^4\Omega^4 k + 356\Omega^6 C_2^4 hNC_1 - 1494N^2 C_1^2 hC_2^3\Omega^4 + \\ & 2808N^3 C_1^3 hC_2^2\Omega^2 + 18NC_1^3 C_2^4 h\Omega^4 - 54N^2 C_1^4 C_2^3 h\Omega^2 - 891N^4 hC_1^4 k + 324N^3 hC_1 C_2\Omega^2 k + 7776N^5 C_1^3 - \\ & 288N^2\Omega^6 C_2^3 - 32\Omega^8 C_2^5 h + 5508N^5 C_1^3 h + 2592N^3 C_1 C_2^2\Omega^4 - 288N^2\Omega^6 C_2^3 h - 7776N^4\Omega^2 C_1^2 C_2 + \\ & 384NC_1\Omega^6 C_2^4 - 1998N^4 hC_1^4 C_2 + 54N^3 C_1^5 C_2^2 h - 2C_1^2 C_2^5 h\Omega^6 - 216N^2 C_1^2 C_2^2 h\Omega^2 k + 6NC_1^3 hC_2^3\Omega^2 k + \\ & 36NC_1\Omega^4 C_2^3 hk + 3456C_2^2 N^3 C_1^3\Omega^2 - 2592N^4 C_1^4 C_2 - 6264N^4 C_1^2 C_2 h\Omega^2 + 2340C_2^3 N^3 C_1\Omega^4 h - 32\Omega^8 C_2^5 \\ & -1728N^2 C_1^2 C_2^3\Omega^4\Bigg] / \\ & \left[C_2\left(-\Omega^6 C_2^3 + 9\Omega^4 C_2^2 C_1 N - 27C_2 N^2\Omega^2 C_1^2 + 27N^3 C_1^3\right) \times (-\Omega^2 C_2 + 3NC_1) \times \sqrt{-\frac{-\Omega^2 C_2 + 3NC_1}{C_2}}\right], \end{aligned} \tag{74b}$$

in which:

$$k = \sqrt{-\frac{-\Omega^2 C_2 + 3C_1 N}{C_2}} \times \sqrt{-C_2(-\Omega^2 C_2 + 3C_1 N)}. \tag{75}$$

Therefore, $u_2(\tau)$ is obtained as follows:

$$u_2 = \frac{3}{8}\frac{hk_1}{\omega_0^2}\sin(\tau) + \frac{1}{8\omega_0^2}\left[8a_2\omega_0^2 + hk_2\right]\cos(\tau) - \frac{h}{8\omega_0^2}\left[k_1\sin(3\tau) + k_2\cos(3\tau)\right], \tag{76}$$

where

$$k_1 = \frac{1}{128\omega_0^2}[12C_1\omega_0 Nha_0^3 + 4\Omega^2 ha_0^3 C_2\omega_0 - 96C_2 a_0^2\omega_0^3 a_1 - 36C_2 a_0^3\omega_0^3 h - 32C_2 a_0^3\omega_1\omega_0^2 - 32C_2 a_0^3\omega_0^3], \quad (77a)$$

$$k_2 = \frac{1}{128\omega_0^2}[-3N^2 ha_0^5 + 96Na_0^2 a_1\omega_0^2 + 36Nha_0^3\omega_0^2 - 4\Omega^2 Nha_0^3 - 3C_2{}^2 a_0^5 h\omega_0^2 + 12C_1 hC_2 a_0^3\omega_0^2 + 32Na_0^3\omega_0^2]. \quad (77b)$$

6 NUMERICAL RESULTS AND DISCUSSION

Based on the HAM, the nonlinear frequency and critical fluid velocity of the embedded Y-SWCNT are obtained in this study. The dimensions and properties used in numerical results for Y-SWCNT are taken as follows [33]: Young's modulus of $E = 1TPa$, the inner radius $R_i = 3.4nm$, the thickness $h_t = 0.34nm$ and $\beta = 0.5$, $\beta_f = 0.01$ and $\beta_{fe} = 0.02$. The harmonic time history of the dimensionless transverse displacement of the Y-SWCNT is shown in Fig. 4. The results of the HAM are validated with Runge-Kutta method and good agreement can be seen between them.

Influences of surrounded elastic medium on the dimensionless natural frequency of the Y-SWCNT are depicted in Figs. 5 and 6. From Fig. 5, it is observed that the dimensionless nonlinear frequency is increased with increasing the elastic medium constants. It is due to the fact that increasing the elastic medium constants increases the stiffness of the structure which yields higher nonlinear frequency values. It is worth mentioning that Pasternak foundation is more effective than Winkler foundation in order to enhance the stability of the nano-tube. This is due to the fact that the Winkler foundation describes the effect of the normal stress of the elastic medium, while Pasternak elastic foundation describes the effects of both tangential and normal stresses of the elastic medium.

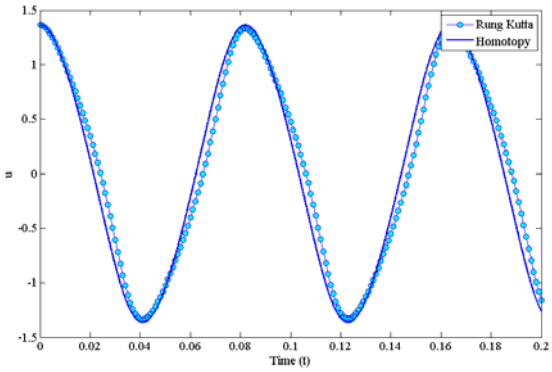

Fig. 4
Time history of the dimensionless transverse displacement obtained from HAM and Runge-Kutta method.

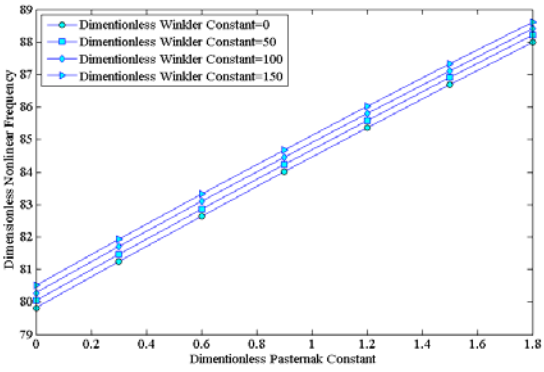

Fig. 5
Effects of Winkler and Pasternak constants on the dimensionless nonlinear frequency.

The nonlinearity and damping effects of Visco- Pasternak elastic medium is demonstrated in Figs. 6. It is seen from Fig. 6(a) that increasing the absolute value of C_1 increases the maximum and minimum values and also decreases the period of u. Fig. 6(b) depicts the effects of C_2. It can be observed that results concluded from C_2 are different from those obtained from C_1. Increasing the values of C_2 decreases the absolute values of maximum and minimum of u.

Variation of dimensionless nonlinear frequency versus the parameter β for different values of dimensionless fluid velocity is illustrated in Fig. 7. It is seen that dimensionless nonlinear frequency of Y-SWCNT decreases as the dimensionless fluid velocity increases. Also, it can be found form Fig.7 that increasing β decreases the dimensionless nonlinear frequency. Therefore, one can say that as the mass of fluid is increased the frequency of the Y-SWCNT decreases and the system becomes more unstable.

The effect of (Kn) on the dimensionless nonlinear frequency of the Y-SWCNT is demonstrated in Fig. 8. It is shown that the frequency is significantly influenced by the *Kn* and the small-size effects of the flow field on the stability characteristics of the nanotubes cannot be ignored. As can be seen, the nonlinear frequency, therefore, the stability of the system is decreased with increasing the (Kn). Moreover, increasing the nonlocal parameter decreases the dimensionless nonlinear frequency. This is because increasing the nonlocal parameter implies decreasing interaction force between nanotube atoms, and that leads to a looser structure.

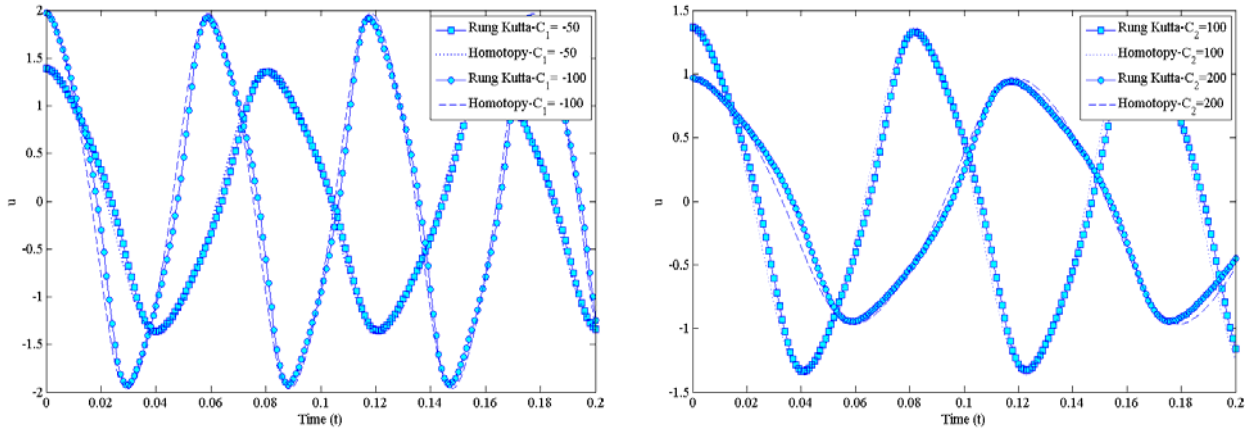

(a) (b)

Fig. 6

a) Time history of the dimensionless transverse displacement obtained from HAM and Runge-Kutta method for various C_1 values. b)Time history of the dimensionless transverse displacement obtained from HAM and Runge-Kutta method for various C_2 values.

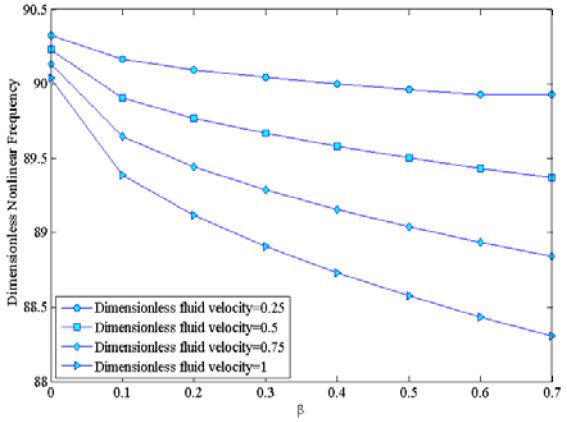

Fig. 7

Dimensionless nonlinear frequency versus β for different values of dimensionless fluid velocities.

In realizing the influence of the angle between centerline of the CNT and the downstream elbows, Fig. 9, shows how dimensionless natural frequency changes with respect to the β. When $\phi = 0$, one can assumes the Y-SWCNT as a cantilevered nanotube without any junction and therefore the fluid goes straight along the length of CNT. As the angle between centerline of the CNT and the downstream elbows increases the frequency of the Y-SWCNT increases which means the system becomes more stable. Fig.10 depicts the dimensionless nonlinear frequency with respect to the strength of dimensionless longitudinally magnetic field for various dimensionless fluid velocities. It can be found from Fig. 10 that increasing the strength of magnetic field increases the nonlinear frequency of the system linearly. Therefore, the system becomes stiffer more stable with increasing the strength of magnetic field.

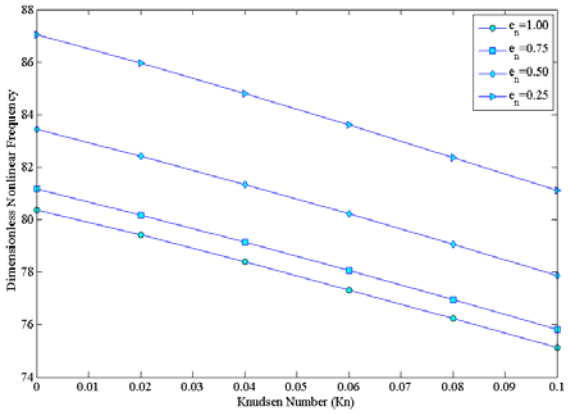

Fig. 8
Dimensionless nonlinear frequency versus (Kn) for different values of dimensionless fluid velocities.

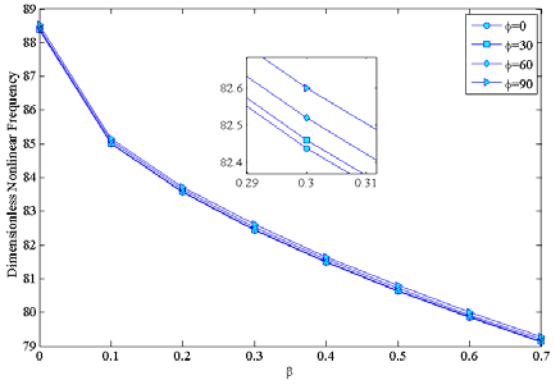

Fig. 9
Dimensionless nonlinear frequency versus β for different values of ϕ.

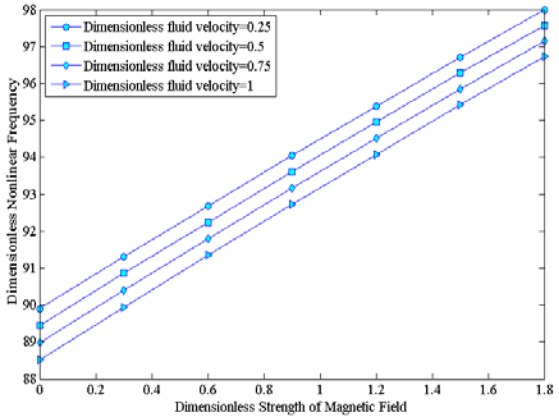

Fig. 10
Dimensionless nonlinear frequency versus dimensionless strength of magnetic field for different values of dimensionless fluid velocities.

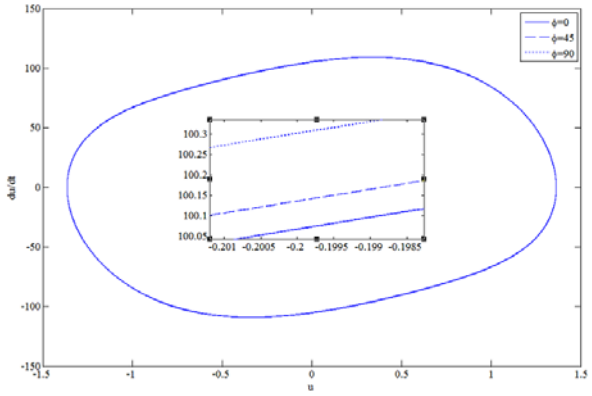

Fig. 11
Phase portrait diagram of the system for different values of ϕ .

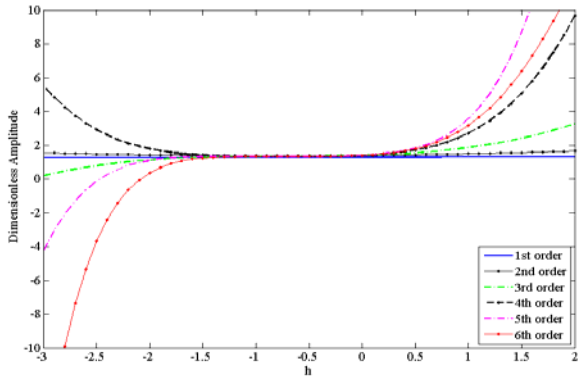

Fig. 12
The effects of the auxiliary parameter h on the dimensionless amplitude.

Fig. 11 illustrates the velocity of each point with respect to its position for different values of angle between the centerline of carbon nanotube and the downstream elbows. It is seen that increasing the angle between the centerline of the CNT and the downstream elbows increases the velocity of each point.

Effects of the auxiliary parameter h on the dimensionless amplitude are illustrated in Fig. 12 for different order approximation of HAM solution. As can be seen, the dimensionless amplitude becomes dependent of h values with increasing the order of approximation. It is also found that for near $-1 < h < -0.5$, dimensionless amplitude converges to the same value.

7 CONCLUSIONS

Based on nonlocal elasticity theory and EBB theory, the vibration behaviors of an embedded Y-SWCNT conveying viscous fluid were studied. The small-size effects and slip boundary conditions of nano-flow through (Kn) were considered. The Y-SWCNT was subjected to a longitudinally magnetic field and also was surrounded by a nonlinear Visco-Pasternak foundation. The Galerkin method as well as HAM was applied to solve the differential equation of motion. The time history of the Y-SWCNT was shown using the HAM and Runge–Kutta methods. The following results may be obtained from this study:

- Implementing nonlocal elasticity theory decreases the nonlinear frequency; therefore the small size effects cannot be neglected.
- Increasing Winkler and Pasternak constants increases the stability of the system.
- Results indicate that the stability of the system is significantly influenced by the (Kn) of fluid flow. The nonlinear frequency of the system decreases with increasing (Kn) of fluid flow.
- The Y-SWCNT becomes more stable by increasing the angle between the centerline of the CNT and the downstream elbows

- Increasing the absolute value of C_1 increases the maximum and minimum values and also decreases the period of u.

ACKNOWLEDGMENTS

The authors would like to thank the referees for their valuable comments. The authors are grateful to University of Kashan for supporting this work by Grant no. 65475/63.

REFERENCES

[1] Iijima S., 1991, Helical microtubules of graphitic carbon, *Nature* **354**:56-58.
[2] Wang B.L., Wang K.F., 2013, Vibration analysis of embedded nanotubes using nonlocal continuum theory, *Composites Part B* **47**:96-101.
[3] Fang B., Zhen Y.X., Zhang C.P., Tang Y., 2013, Nonlinear vibration analysis of double-walled carbon nanotubes based on nonlocal elasticity theory, *Applied Mathematical Modelling* **37**:1096-1107.
[4] Simsek M., Yurtcu H.H., 2013, Analytical solutions for bending and buckling of functionally graded nanobeams based on the nonlocal Timoshenko beam theory, *Composite Structures* **97**:378-386.
[5] Liang F., Su Y., 2013, Stability analysis of a single-walled carbon nanotube conveying pulsating and viscous fluid with nonlocal effect, *Applied Mathematical Modelling* **37**:6821-6828.
[6] Ghorbanpour Arani A., Abdollahian M., Kolahchi R., Rahmati A.H., 2013, Electro-thermo-torsional buckling of an embedded armchair DWBNNT using nonlocal shear deformable shell model, *Composites Part B* **51**:291-299.
[7] Ke L.L., Wang Y.S., Wang Z.D., 2012, Nonlinear vibration of the piezoelectric nanobeams based on the nonlocal theory *Composite Structures* **94**:2038-2047.
[8] Ghorbanpour Arani A., Kolahchi R., Vossough H., 2012, Buckling analysis and smart control of SLGS using elastically coupled PVDF nanoplate based on the nonlocal Mindlin plate theory, *Physica B* **407**:4458-4465.
[9] Ghorbanpour Arani A., Kolahchi R., Khoddami Maraghi Z., 2013, Nonlinear vibration and instability of embedded double-walled boron nitride nanotubes based on nonlocal cylindrical shell theory, *Applied Mathematical Modelling* **37**:7685-7707.
[10] Ke L.L., Wang Y.S., Yang J., Kitipornchai S., 2012, Nonlinear free vibration of size-dependent functionally graded microbeams, *International Journal of Engineering Science* **50**:256-267.
[11] Asghari M., Kahrobaiyan H.H., Ahmadian M.T., 2010, A nonlinear Timoshenko beam formulation based on the modified couple stress theory, *International Journal of Engineering Science* **48**:1749-1761.
[12] Reddy J.N., 2011, Microstructure-dependent couple stress theories of functionally graded beams, *Journal of the Mechanics and Physics of Solids* **59**:2383-2399.
[13] Chena W., Lili M.X., 2012, A model of composite laminated Reddy plate based on new modified couple stress theory, *Composite Structures* **94**:2143-2156.
[14] Zhao J., Zhou S., Wang B., Wang X., 2012, Nonlinear microbeam model based on strain gradient theory, *Applied Mathematical Modelling* **36**:2674-2686.
[15] Ramezani S., 2012, A micro scale geometrically non-linear Timoshenko beam model based on strain gradient elasticity theory, *International Journal of Non-Linear Mechanics* **47**:863-873.
[16] Eringen A.C., 1983, On differential equations of nonlocal elasticity and solutions of screw dislocation and surface waves, *Journal of Applied Physics* **54**:4703-4710.
[17] Wang L., 2009, Dynamical behaviors of double-walled carbon nanotubes conveying fluid accounting for the role of small length scale, *Computational Materials Science* **45**:584-588.
[18] Ghavanloo E., Daneshmand F., Rafiei M., 2010, Vibration and instability analysis of carbon nanotubes conveying fluid and resting on a linear viscoelastic Winkler foundation, *Physica E* **42**:2218-2224.
[19] Kuang Y.D., He X.Q., Chen C.Y., Li G.Q., 2009, Analysis of nonlinear vibrations of double-walled carbon nanotubes conveying fluid, *Computational Materials Science* **45**:875-880.
[20] Xia W., Wang L., 2010, Vibration characteristics of fluid-conveying carbon nanotubes with curved longitudinal shape, *Computational Materials Science* **49**:99-103.
[21] Wang L., Ni Q., 2009, A reappraisal of the computational modelling of carbon nanotubes conveying viscous fluid, *Mechanics Research Communications* **36**:833-837.
[22] Abdollahian M., Ghorbanpour Arani A., Mosallaie Barzoki A.A., Kolahchi, R., Loghman A., 2013, Non-local wave propagation in embedded armchair TWBNNTs conveying viscous fluid using DQM, *Physica B* **418**:1-15.
[23] Lee H.L., Chang W.J., 2009, Vibration analysis of a viscous-fluid-conveying single-walled carbon nanotube embedded in an elastic medium, *Physica E* **41**:529-532.
[24] Jannesari H., Emami M.D., Karimpour H., 2012, Investigating the effect of viscosity and nonlocal effects on the stability of SWCNT conveying flowing fluid using nonlinear shell model, *Physics Letters A* **376**:1137-1145.

[25] Rashidi V., Mirdamadi H.R., Shirani E., 2012, A novel model for vibrations of nanotubes conveying nanoflow, *Computational Materials Science* **51**:347-352.
[26] Mirramezani M., Mirdamadi H.R., 2012, Effects of nonlocal elasticity and Knudsen number on fluid–structure interaction in carbon nanotube conveying fluid, *Physica E* **44**:2005-2015.
[27] Lei X.W., Natsuki T., Shi J.X., Ni Q.Q., 2012, Surface effects on the vibrational frequency of double-walled carbon nanotubes using the nonlocal Timoshenko beam model, *Composites Part B* **43**:64-69.
[28] Ashgharifard Sharabiani P., Haeri Yazdi M.R., 2013, Nonlinear free vibrations of functionally graded nanobeams with surface effects, *Composites Part B* **45**:581-586.
[29] Wang L., 2010, Vibration analysis of fluid-conveying nanotubes with consideration of surface effects, *Physica E* **43**:437-439.
[30] Biro L.P., Horvath Z.E., Mark G.I., Osvath Z., Koos A.A., Santucci S., Kenny J.M., 2004, Carbon nanotube Y junctions: growth and properties, *Diamond and Related Materials* **13**:241-249.
[31] Lin R.M., 2012, Nanoscale vibration characterization of multi-layered graphene sheets embedded in an elastic medium, *Computational Materials Science* **53**:44-52.
[32] Pradhan S.C., Phadikar J.K., 2009, Small scale effect on vibration of embedded multilayered graphene sheets based on nonlocal continuum models, *Physics Letters A* **373**:1062-1069.
[33] Ghorbanpour Arani A., Zarei M.Sh., Amir S., Khoddami Maraghi Z., 2013, Nonlinear nonlocal vibration of embedded DWCNT conveying fluid using shell model, *Physica B* **410**:188-196
[34] Ghorbanpour Arani A., Amir S., 2013, Electro-thermal vibration of visco-elastically coupled BNNT systems conveying fluid embedded on elastic foundation via strain gradient theory, *Physica B* **419**:1-6.
[35] Eichler A., Moser J., Chaste J., Zdrojek M., Wilson-Rae I., Bachtold A., 2011, Nonlinear damping in mechanical resonators made from carbon nanotubes and grapheme, *Nature Nanotechnology* **6**:339-342.
[36] Pirbodaghi T., Ahmadian M.T., Fesanghary M., 2009, On the homotopy analysis method for non-linear vibration of beams, *Mechanics Research Communications* **36**:143-148.
[37] Moghimi Zand M., Ahmadian M.T., 2009, Application of homotopy analysis method in studying dynamic pull-in instability of Microsystems, *Mechanics Research Communications* **36**:851-858.
[38] Reddy J.N., Wang C.M., 2004, *Dynamics of Fluid-Conveying Beams: Governing Equations and Finite Element Models*, Centre for Offshore Research and Engineering National University of Singapore.
[39] Ghorbanpour Arani A., Amir S., 2013, Nonlocal vibration of embedded coupled CNTs conveying fluid under thermo-magnetic fields via ritz method, *Journal of Solid Mechanics* **5**:206-215.
[40] Gurtin M.E., Murdoch A.I., 1975, A continuum theory of elastic material surfaces, *Archive for Rational Mechanics and Analysis* **57**:291-323.
[41] Narendar S., Ravinder S., Gopalakrishnan S., 2012, Study of non-local wave properties of nanotubes with surface effects, *Computational Materials Science* **56**:179-184.
[42] Paidoussis M.P., 1998, *Fluid-Structure Interactions: Slender Structures and Axial Flow*, Academic Press, London.
[43] Liao S.J., 2003, *Beyond Perturbation: Introduction to the Homotopy Analysis Method*, Chapman and Hall, CRC Press, Boca Raton.
[44] Hosseini S.H., Pirbodaghi T., Asghari M., Farrahi G.H., Ahmadian M.T., 2008, Nonlinear free vibration of conservative oscillators with inertia and static type cubic nonlinearities using homotopy analysis method, *Journal of Sound and Vibration* **316**:263-273.